

# GENERATING POSSIBLE CONFLICTS FROM BOND GRAPHS USING TEMPORAL CAUSAL GRAPHS

Anibal Bregon, Belarmino Pulido  
Department of Computer Science  
University of Valladolid  
Valladolid, 47011, Spain  
Email: {anibal,belar}@infor.uva.es

Gautam Biswas, Xenofon Koutsoukos  
Institute for Software Integrated Systems  
Vanderbilt University  
Nashville, TN 37235, USA  
Email: {gautam.biswas,xenofon.koutsoukos}@vanderbilt.edu

## KEYWORDS

Bond Graphs, Temporal Causal Graph, ARR, Possible Conflicts, Model-based Diagnosis

## ABSTRACT

Accurate modeling mechanisms play an important role in model-based diagnosis, and the bond graph modeling language has proved to be helpful for this task. In this paper we present an algorithm for automatically derive ARR-like structures, possible conflicts, from the bond graph model of a system. The algorithm uses temporal causal graphs as an intermediate structure to generate the set of possible conflicts. Performance of the algorithm for structural and sensor faults is then studied. Finally, we present another algorithm to automatically derive temporal information in the fault signature matrix for the set of possible conflicts, thus improving the isolation capabilities of the approach.

## INTRODUCTION

Fault diagnosis and prognosis mechanisms play an important role in accurate and reliable operation of complex engineering systems. Accurate models play an important role in generating correct diagnosis results. Model-based reasoning approaches use the models as the core element for its reasoning process. Among all these approaches, model-based diagnosis techniques are becoming quite prevalent because of their generality, their applicability across multiple operating regions, and their potential for overcoming the device dependency problem.

An approach that has been successful for modeling the dynamic behavior of physical systems from first principles are bond graphs [Karnopp et al. (2000)]. Bond graphs provide an easy, intuitive way to build multi-domain energy-based models by combining system topology with a small set of component behavior processes. The topological structure of bond graph models also provides the infrastructure for developing effective and efficient fault diagnosis methods based on causal analysis that links component parameters to system variables using well defined methods.

Several approaches have been proposed to carry on the diagnosis process from bond graph models [Mosterman and Biswas (1999); Samantaray and Bouamama (2008)].

In earlier work [Bregon et al. (2008)], we compared some of these approaches against the possible conflicts diagnosis approach [Pulido and Alonso-González (2004)], an ARR-like compilation technique from the Artificial Intelligence Diagnosis (DX) community. In this work we showed the advantages of exploiting causal and temporal relations between process parameters and the measurement variables, provided by temporal causal graphs, for residual generation and analysis. The goal of this paper is to develop an automatic way to exploit these relations within the possible conflicts diagnosis framework.

Main contributions of the paper are as follows: (1) we developed an algorithm to automatically compute the set of possible conflicts for a system from its bond graph model using temporal causal graphs, i.e., minimal sets of equations that can be used for diagnosis purposes, (2) PCs and ARRs use different minimality concepts, the proposed algorithm allows to automatically generate the set of possible conflicts which include the set of structurally independent ARRs, but also additional PCs which can be used for sensor fault isolation, and (3) we propose an algorithm to automatically generate the fault signature matrix of the set of possible conflicts including temporal information.

The rest of the paper is organized as follows. The next section briefly describes the bond graph approach. A three tank system is used to illustrate the modeling approach. This is followed by a discussion of the possible conflicts approach to diagnosis. The following section presents the algorithm to automatically derive the set of possible conflicts from the bond graph model of a system. The basis for the possible conflicts' fault signature matrix generation with temporal information are presented. Next, results for the case study of a nonlinear, controlled three tank system are shown. Finally, the last section presents conclusions and future work.

## BOND GRAPH MODELING

Bond graphs are labeled, directed graphs, that present a topological, domain-independent, energy-based methodology for modeling the dynamic behavior of physical systems [Karnopp et al. (2000); Samantaray and Bouamama (2008)]. Building system models follows an intuitive approach where energy flow paths between system components are captured by a topological structure

where system components appear as nodes, and the energy flow paths appear as links or bonds. We will use the laboratory plant model of a three tank system (shown in fig. 1) to illustrate the significant concepts in this paper.

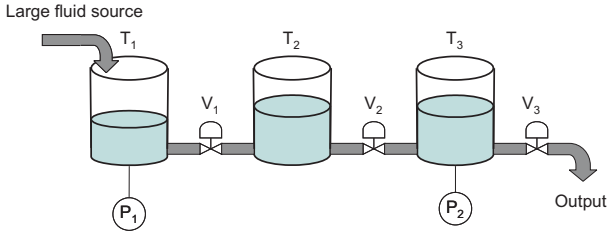


Figure 1: Three-tank system.

Fig. 2 shows the bond graph model for the plant. The tanks are modeled as capacitors that hold fluid, and the valves and pipes as resistances to flow. 0- and 1- junctions represent the common effort (i.e., pressure) and common flow (i.e., flowrate) points in the system, respectively. Measurement points, shown as De components, are connected to junctions, and the faults appear as explicit parameters of the bond graph model.

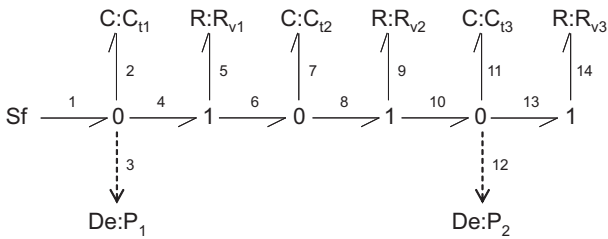


Figure 2: Bond graph model of the plant including the effort measurements ( $De : P_1, De : P_2$ )

This representation provides a systematic framework for capturing causal relations between system variables, i.e., causal graphs can easily be automatically derived from bond graph models. A special class of causal graph, is the Temporal Causal Graph, that captures not only the causal, but also the temporal relations between system variables.

### Deriving Temporal and Causal Relations: the Temporal Causal Graph

Temporal Causal Graphs, TCG, defined by Mosterman and Biswas [Mosterman and Biswas (1999)] for diagnosis tasks, are an extended form of signal flow graphs for dynamic systems, that capture the causal and temporal relations between process parameters and the measurement variables in the system. More formally, a TCG can be defined as [Roychoudhury et al. (2006)]:

**Definition 1** (Temporal Causal Graph). A TCG is a directed graph  $\langle V, L, D \rangle$ .  $V = E \cup F$ , where  $V$  is a set of vertices,  $E$  is a set of effort variables and  $F$  is a set of flow variables in the bond graph system model.  $L$  is the

label set  $\{=, 1, -1, p, p^{-1}, p dt, p^{-1} dt\}$  ( $p$  is a parameter name of the physical system model). The  $dt$  specifier indicates a temporal edge relation, which implies that a vertex affects the derivative of its successor vertex across the temporal edge.  $D \subseteq V \times L \times V$  is a set of edges [Narasimhan and Biswas (2007)].

TCGs can be directly derived from bond graph models, with effort and flow variables represented as vertices, and relations between the variables represented as directed edges.

Fig. 3 shows the TCG for the three tank system. Junctions and resistors define instantaneous magnitude relations, and capacitors and inertias define temporal effects on causal edges.

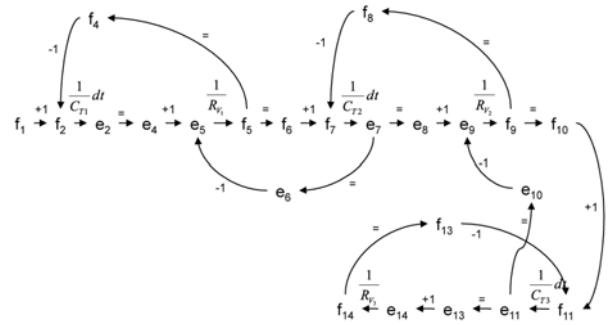


Figure 3: Temporal causal graph of the three tank system.

### POSSIBLE CONFLICTS DIAGNOSIS APPROACH

Consistency based approaches are commonly employed in model-based diagnosis methods employed by the Artificial Intelligence community. Possible conflicts, PCs for short [Pulido and Alonso-González (2004)], are those sub-systems that may become conflicts when faults occur within the Consistency Based Diagnosis framework [Reiter (1987)], i.e., *minimal subsets of equations containing the analytical redundancy necessary to perform fault diagnosis* [Pulido and Alonso-González (2004)].

Computation of PCs is performed on an abstract model linked to the set of equations in the system description, i.e., a hypergraph including just the constraints in the model, and their related known and unknown variables. PCs are derived off-line using two core concepts: *minimal evaluation chains*, or MECs, and *minimal evaluation models*, or MEMs.

MECs are minimal over-constrained sets of relations, and they represent a necessary condition for a conflict to exist. MECs represent a partial subhypergraph from the original system description.

Each constraint in a MEC has one or more variables, and each variable could be solved using the constraint, assuming the remaining variables are known. This fact is called an interpretation for the constraint, i.e. a feasible causal assignment. In the general case, not every interpretation is feasible for non-linear dynamic models.

The set of interpretations, seen as causal links among variables in each hyper-arc, define a causal graph for each MEC. A MEM is a global consistent causal interpretation for every constraint in a MEC. Hence, a MEM is a subgraph for each MEC. Using the whole set of available interpretations for each constraint in a MEC, algorithms used to compute PCs are able to find every possible causal interpretation which is globally consistent within a MEC, i.e., the whole set of MEMs for each MEC. Each MEM describes an executable model, which can be used to perform fault detection. Possible Conflicts are defined as the set of relations in a MEC that has, at least, one MEM.

If there is a discrepancy between predictions from these models and current observations, the PC must be responsible for such a discrepancy, and should be confirmed as a real conflict. Afterwards, diagnosis candidates are obtained from conflicts following Reiter’s theory. Further information concerning PC calculation can be found in [Pulido and Alonso-González (2004)].

PCs calculation uses a minimality criteria in terms of sets of constraints. Nevertheless, it is straightforward to obtain candidates based on components. As pointed out in [Pulido and Alonso-González (2004)], the set of MEMs generated with this approach is equivalent to the set of conflicts computed by the GDE.

Moreover, if algorithms used to compute ARR through structural analysis use such minimality criterion and provide a complete solution –explores every possible causal assignment for every minimal ARR–, the set of PCs has same detection and isolation capabilities as the set of minimal ARRs.

Finally, if every MEM in every PC provides the same solution –what is called the *Equivalence assumption* in [Pulido and Alonso-González (2004)]–, then PCs, minimal ARRs, and minimal conflicts provide the same solution in terms of fault detection and isolation capabilities.

Cordier et al. [Cordier et al. (2004)] introduced the concept of *support* for an ARR (set of components whose models are used to derive an ARR). Based on such idea, off-line compiled conflicts and ARR’s support can be considered as equivalent (the support for an ARR is a potential conflict, which is equivalent to a possible conflict [Cordier et al. (2004); Pulido and Alonso-González (2004)]). Under given conditions, the set of minimal ARRs and the set of minimal conflicts will have same detection and isolation capabilities.

Once minimal PCs of a system have been identified, the next step deals with establishing the set of PCs that would be activated in presence of each fault, i.e., the fault signature matrix, FSM. The FSM relates faults that can occur in the system with PCs that would be activated for each fault.

For the three tank plant, two PCs are derived. Table 1 shows the resulting fault signature matrix. Columns  $PC_1$  and  $PC_2$  show the theoretical activation values of the PCs in presence of the different kind of faults considered (shown in the first column). Column  $I$  shows the

isolation capabilities of the approach.

	$PC_1$	$PC_2$	$I$
$C_{T_1}$	1	0	1
$C_{T_2}$	1	1	0
$C_{T_3}$	0	1	0
$R_{V_1}$	1	1	0
$R_{V_2}$	1	1	0
$R_{V_3}$	0	1	0

Table 1: Signature matrix of the possible conflicts found for the three tank system.

Current implementation of PCs computation needs the hypergraph and the interpretation for each hyper-arc to be provided by the user. In this work we employ the structural, causal and temporal information provided by the TCGs derived from the bond graphs, to automatically compute the set of PCs from a given system description. The only requirement is to have the system description as a bond graph.

## PC DERIVATION FROM BOND GRAPHS

In this section we present an algorithm to automatically derive the set of PCs from the bond graph model of a system. Similar approaches have already been proposed in the literature for the same purpose. Samantaray et al. [Samantaray and Bouamama (2008); Samantaray et al. (2006)] introduced the Diagnostic Bond Graphs, DBG, as a way to obtain all the ARRs of a system. The problem with this approach is that it requires a previous process of causality inversion in the sensors, what makes it difficult to automate the whole process of ARR generation. Other approaches, like [Bouamama and Samantaray (2003)], present the steps that must be followed to generate the set of ARRs, but no algorithm is provided.

Moreover, as shown in [Bregon et al. (2008)], the PCs diagnosis approach exhibits some advantages against the ARRs approach. While ARRs/DBGs are designed to use derivative causality in the system [Samantaray and Bouamama (2008)], PCs are designed to automatically work with both integral or derivative causality. Another important difference is that ARRs consider that discrepancies in the system can only be found comparing an estimated variable against a measured one. PCs, on the other side, consider that discrepancies in the system are found comparing an estimated variable against a measured variable, or just comparing two variables that can be estimated by means of the measured ones.

To compute the set PCs we need to look for MECs with at least one MEM. MEMs can be derived while finding MECs, just checking global consistency of the causal graph w.r.t. the causal assignments. Temporal causal graphs are pretty suitable for this purpose, because are able to provide all the causal paths from a variable to the sensors or sources. Moreover, TCGs will provide the system with temporal information that, as we will see later, can be used to improve the isolation capabilities of the

approach. Therefore, we will use TCGs as an intermediate step for PCs computation from bond graphs.

Algorithms to automatically derive the TCG from the bond graph model can be found in the literature [Mosterman and Biswas (1999)]. Once the TCG has been derived, we have to clearly mark the following items within the TCG model in order to derive MEMs:

- Sensors in the system, i.e., measured variables.
- Discrepancy nodes, i.e., measured, and non-measured variables in the TCG whose value can be estimated by two independent incident edges.

Algorithm 1 is invoked on the temporal causal graph to obtain the set of possible conflicts of the system. For every discrepancy node, this algorithm invokes algorithm 2. Algorithm 2, is a recursive algorithm that propagates backward along the directed edges of the temporal causal graph trying to eliminate all unknown variables from the discrepancy node. When all unknown variables are eliminated by means of measured variables ( $vertex == \emptyset$ ), a PC has been found, and minimality conditions have to be checked. If the PC is minimal w.r.t. the rest of the PCs found in the system, the PC is added to the set of PCs,  $SPC$ ; if not, the PC is discarded. An example of its application from the discrepancy node  $e_2$  (that is measured and can also be estimated) is shown in fig. 4.

---

**Algorithm 1:** For each discrepancy node,  $dn$ , marked in the TCG, we try to find any possible conflict,  $pc$ ;  $SPC$  is the set of possible conflicts;  $SDN$  is the set of discrepancy nodes

---

```

1 function SPC := find_every_pc_for_each_dn (SDN)
2 foreach  $dn$  in  $SDN$  do
3    $vertex = \{dn\}$ ;
4   find_pc( $vertex, \{\}, SPC$ )
5 end

```

---

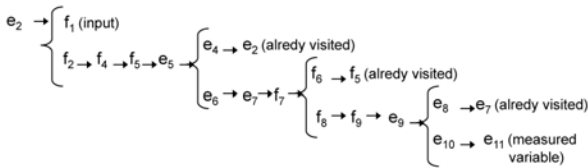


Figure 4:  $PC_1$  derivation by means of algorithm 2 for  $find\_pc(\{e_2\}, \{\}, SPC)$

Looking at the TCG for the running example (fig. 2) the reader can see that a PC can be obtained propagating backwards through the TCG from the discrepancy node  $e_2$ . The backward propagation will stop when all the unknown variables become explained. In this example, when the backward propagation reaches the measured variable  $e_{11}$ , the algorithm will stop and identify a possible conflict (see figure 4). Another PC can be found propagating backwards in the TCG from the discrepancy node

---

### Algorithm 2:

---

```

1 function find_pc ( $vertex, pc, SPC$ )
2 if  $vertex == \emptyset$  then
3   if  $pc$  is not in  $SPC$  and  $pc$  is minimal then
4     insert  $pc$  in  $SPC$ ;
5   end
6 else
7   foreach  $v'$  in  $vertex$  do
8      $vertex = vertex \setminus \{v'\}$ ;
9     foreach ancestor  $av'$  needed to compute  $v'$  do
10      if  $av'$  has not been visited then
11        if  $av'$  is a source or a sensor then
12           $pc = pc \cup \{av'\}$ ;
13        else
14           $vertex = vertex \cup \{av'\}$ ;
15           $pc = pc \cup \{av'\}$ ;
16        end
17      end
18      find_pc( $vertex, pc, SPC$ );
19    end
20 end

```

---

$e_{11}$  until the measured variable  $e_2$  is reached. To find both PCs, we have considered the observational model of the system implicitly included in the TCG, i.e.,  $e_2$  and  $e_{11}$  are directly marked as measured variables. But, what happens when the observational model is explicitly included in the TCG?

### Extension to Sensor Faults

As Bouamama et al. claim [Bouamama and Samantaray (2003)], in presence of multiple sensors, if some residuals share common variables, linear combinations of these residuals can produce independent residuals. Although it is quite clear that these residuals cannot provide additional structural isolation capabilities to the diagnosis system, they can be used for sensor fault isolation. One of the advantages of the proposed algorithms is that just slight changes in the TCG need to be made:

- TCG have to be modified in such a way that the observational model of the system becomes explicitly included.

For the three tank running example, sensor variables  $s_1$  and  $s_2$  have to be included in the TCG. Now, variables  $e_2$  and  $e_{11}$  could be either estimated or measured. Fig 5 shows the extended TCG for the three tank system example.

Following with the three tank running example, if we invoke algorithms 1 and 2 on the extended TCG (fig. 5) from the discrepancy node  $e_2$ , we obtain: (1), the same PC that we previously obtained ( $PC_1$ ) if the path from  $e_{11}$  to the sensor  $s_2$  is followed (see upper part of fig. 6); and (2), a new PC if the path from  $e_{11}$  to the variable  $f_{11}$  (and further backward propagation) is followed (see lower part of fig. 6). In terms of minimality criteria,

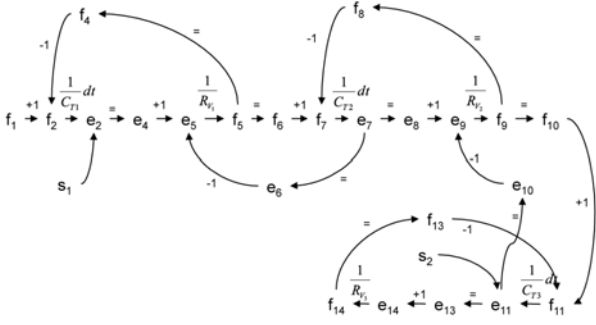


Figure 5: Extended temporal causal graph of the three tank system.

the new PC will be minimal w.r.t the other PC because now we are considering sensor equations as part of the system, and consequently, the new PC is not maximal from the already existing PC (because does not include the sensor equation).

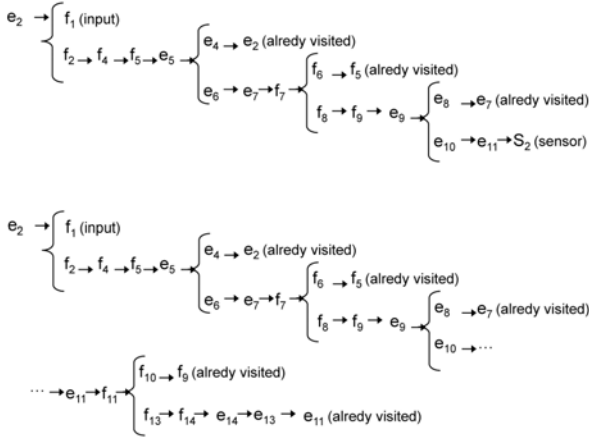


Figure 6:  $PC_1$  (upper part) and additional  $PC_3$  (lower part) for the first sensor obtained using the modified algorithm 2.  $PC_1$  explains the variable  $e_{11}$  propagating backwards through the edge to the measured variable  $s_2$ . The additional  $PC_3$  explains the variable  $e_{11}$  propagating backwards through the edge to the variable  $f_{11}$ .

Table 2 shows the resulting signature matrix for the extended version of the algorithm. Columns show the theoretical activation values of the PCs in presence of the different kind of faults considered (shown in the first column). Columns  $PC_1$  and  $PC_2$  show the original PCs found in the system (also found with the new version of the algorithm). Column  $I_1$  shows the isolation capabilities these two PCs. Columns  $PC_3$  and  $PC_4$  show the additional PCs obtained for the system, and column  $I_2$  shows the isolation capabilities of the approach for the whole set of PCs. Additional rows have been added to the FSM for each of the sensor faults considered. Looking at columns  $I_1$  and  $I_2$ , it is clear that using the original set of PCs, sensor faults cannot be isolated, but if the whole set of PCs is used, both sensor faults can be isolated.

	$PC_1$	$PC_2$	$I_1$	$PC_3$	$PC_4$	$I_2$
$CT_1$	1	0	1	1	1	1
$CT_2$	1	1	0	1	1	0
$CT_3$	0	1	0	1	1	0
$RV_1$	1	1	0	1	1	0
$RV_2$	1	1	0	1	1	0
$RV_3$	0	1	0	1	1	0
$S_1$	1	1	0	1	0	1
$S_2$	1	1	0	0	1	1

Table 2: Signature matrix for the whole set of possible conflicts found for the three-tanks system.

## THE REDUCED QUALITATIVE FAULT SIGNATURE MATRIX

Given current observations, residual for PCs and ARRs, should provide values in presence of the different kind of faults as 1 if the residual is activated, or 0 if it is not activated. Recently, several authors [Koscielny (1995); Koscielny and Zakroczymski (2000); Puig et al. (2005); Gelso et al. (2008)] have proposed extensions to improve the fault detection and isolation stages based on ARRs or PCs, including temporal information about residuals. The problem is that such extensions are hard to obtain automatically.

The qualitative fault signatures approach from Mosterman and Biswas [Mosterman and Biswas (1999)] uses the properties of TCGs to automatically derive the FSM of a system including temporal information (known as the qualitative fault signature matrix, QFSM). Given a set of faulty parameters and a set of measurements associated with a system, the qualitative fault signatures can be derived from the TCG model of the system by forward propagation from the fault parameter along the edges of the TCG to the measurement nodes [Mosterman and Biswas (1999)].

Our proposal consists in applying a TRANSCEND-like forward propagation algorithm to automatically obtain the qualitative fault signature matrix for each of the PCs of a system. As we used the TCG to generate the set of PCs, we can now use the TCG model of each PC to propagate forward from the fault parameter along the edges to the discrepancy nodes of the PCs to obtain a FSM with temporal information. We will call this matrix, the reduced qualitative fault signature matrix (RQFSM).

The method for predicting future behavior is shown in algorithm 3. The algorithm uses the TCG model of each PC to find the signatures. For each hypothesized fault that can activate a PC, the algorithm invokes TRANSCEND's prediction algorithm [Mosterman and Biswas (1999)] using only the TCG model of the PC. This prediction algorithm [Mosterman and Biswas (1999)] will compute, in a qualitative way, the behavior of the discrepancy nodes of the PCs, i.e., the behavior of the PC. This behavior is expressed in terms of the magnitude (zeroth order time-derivative), slope (first order time-derivative), and higher order effects. All deviation propagations start off as zeroth order effects (magnitude changes). When an integrating edge in the TCG

is traversed, the magnitude change becomes a first order change, i.e., the first derivative of the affected quantity changes.

**Algorithm 3:** For each possible conflict's TCG,  $TCG_{PC_X}$ , we find the signatures for all hypothesized faults using a TRANSCEND-like prediction algorithm; SPC is the set of possible conflicts

```

1 function RQFSM := find_rqfsm(SPC)
2 foreach  $PC_X$  in SPC do
3   foreach fault candidate in  $PC_X$  do
4     Predict_Future_Behavior_Algorithm( $TCG_{PC_X}$ ,
      fault candidate)
5   end
6 end

```

Algorithm 3 returns the signature of all hypothesized fault for each PC. It is important to point out that TRANSCEND's algorithm can not be directly used to get the RQFSM of a system, because the algorithm has to be invoked as many times as PCs have been found in the system, and for the parts of the TCG related with the PCs.

Table 3 shows the reduced qualitative fault signature matrix for the three tank plant. Columns  $PC_1$  and  $PC_2$  represent the expected deviations (no change (0), or increasing or decreasing (+/-)) in the magnitudes, and in the slope or higher order effects, in the presence of faults for each possible conflict. Column  $I$  shows isolation capabilities of this approach. Column  $I$  clearly shows the increment in the discrimination power compared with previous approaches, due to the inclusion of temporal information (in magnitudes, slopes and higher order effects) in the theoretical FSM.

	$PC_1$	$PC_2$	$I$
$C_{T_1}$	-+		1
$C_{T_2}$	0-	0-	1
$C_{T_3}$		+ -	1
$R_{V_1}$	0+	0-	0
$R_{V_2}$	0+	0-	0
$R_{V_3}$		0+	1

Table 3: RQFSM found for the three tank system.

## CASE STUDY

The laboratory plant shown in fig. 7 will be used to study the proposed algorithms. This plant resembles common features of a continuous industrial process. It is made up of three tanks  $\{T_1, T_2, T_3\}$ . A control loop defined by a function  $f(x)$ , where  $x$  is the pressure in tank  $T_1$ , determines the opening of valve  $V_0$ . Valves  $V_1$ ,  $V_2$ , and  $V_3$  are completely open. We assume four sensors: two,  $\{P_1, P_2\}$ , measure the fluid pressure in tanks  $T_1$  and  $T_3$ , the third,  $\{F_1\}$ , measures the in-flow into tank  $T_1$ , and the fourth,  $\{F_2\}$ , measures the outflow from tank  $T_3$ . For this study, we consider seven different parametric faults in the plant: change in tanks  $T_1, T_2, T_3$  capacities, and

block in valves  $V_1, V_2, V_3$ , and in the input pipe. We also consider sensor faults.

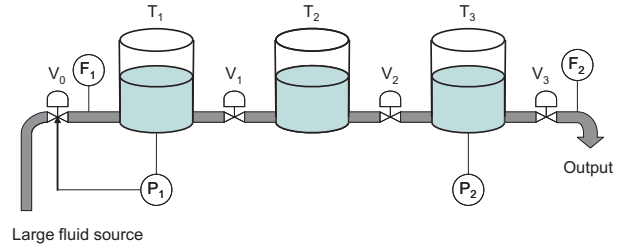


Figure 7: Diagram of the laboratory plant.

Fig. 8 shows the bond graph model for the plant. Measurement points shown as De and Df components are connected to junctions, and the faults listed above, appear as explicit parameters of the bond graph model. Fig. 9 shows the TCG for the plant.

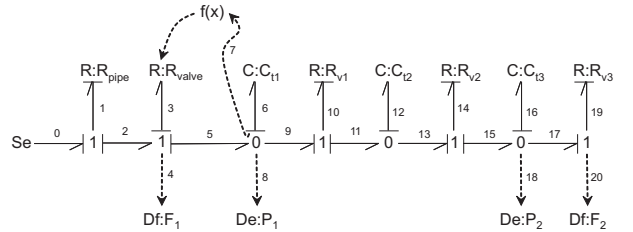


Figure 8: Bond graph model of the plant. Here,  $f(x)$  represents the function of the pressure in  $T_1$  that controls the resistance  $R_{valve}$  (control on the aperture of  $V_0$ ).

## Results for the Case Study

Invoking algorithms 1 and 2 from the three tank plant's TCG we automatically obtained a set of four possible conflicts. Table 4 shows the FSM for this set of PCs. Columns  $PC_1, PC_2, PC_3$ , and  $PC_4$  show the theoretical activation values of the PCs in presence of the different kind of faults considered (shown in the first column). Column  $I$  shows the isolation capabilities of the approach. Results for this plant are equivalent to those obtained using the the ARR/DBG approach for the same model (as stated in [Bregon et al. (2008)]).

	$PC_1$	$PC_2$	$PC_3$	$PC_4$	$I$
$C_{T_1}$	0	1	0	0	1
$C_{T_2}$	0	1	1	0	0
$C_{T_3}$	0	0	1	0	1
$R_{V_1}$	0	1	1	0	0
$R_{V_2}$	0	1	1	0	0
$R_{V_3}$	0	0	0	1	1
$R_{pipe}$	1	0	0	0	1

Table 4: Signature matrix of the possible conflicts found for the laboratory plant.

If sensor faults are considered, we can invoke the extended version of algorithm 2. With this approach, we obtained a set of 15 minimal PCs for the system. Table 5 shows the fault signature matrix for these 15 PCs.

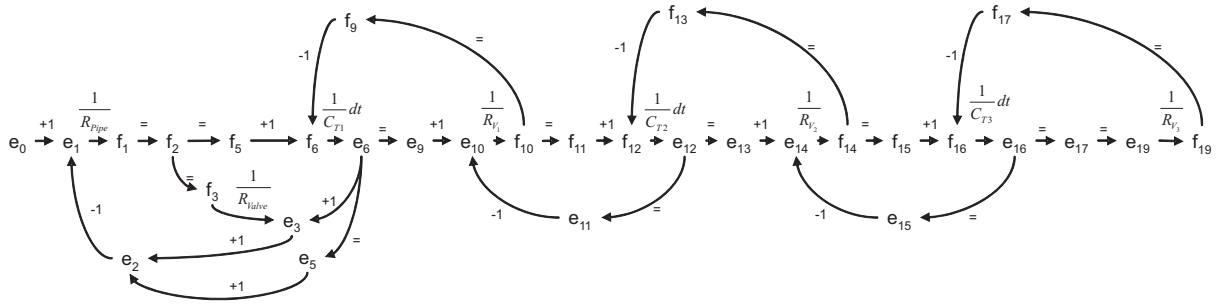


Figure 9: Temporal causal graph of the three tank plant.

	$PC_1$	$PC_2$	$PC_3$	$PC_4$	$I_1$	$PC_5$	$PC_6$	$PC_7$	$PC_8$	$PC_9$	$PC_{10}$	$PC_{11}$	$PC_{12}$	$PC_{13}$	$PC_{14}$	$PC_{15}$	$I_2$
$C_{T1}$	0	1	0	0	1	1	1	1	1	1	1	1	1	1	0	0	1
$C_{T2}$	0	1	1	0	0	1	1	1	1	1	1	1	1	1	1	1	0
$C_{T3}$	0	0	1	0	1	0	1	0	1	1	1	1	1	1	1	1	1
$R_{V1}$	0	1	1	0	0	1	1	1	1	1	1	1	1	1	1	1	0
$R_{V2}$	0	1	1	0	0	1	1	1	1	1	1	1	1	1	1	1	0
$R_{V3}$	0	0	0	1	1	0	0	0	0	0	1	1	0	1	1	1	1
$R_{pipe}$	1	0	0	0	1	1	1	1	1	1	1	1	0	0	0	0	1
$F_1$	1	1	0	0	0	1	1	0	0	0	0	0	1	1	0	0	1
$P_1$	1	1	0	0	0	0	0	1	1	0	0	0	1	0	1	1	1
$P_2$	0	1	1	1	1	1	0	1	0	1	1	0	0	1	1	0	1
$F_2$	0	0	1	1	1	0	1	0	1	1	0	1	1	0	0	1	1

Table 5: Signature matrix for the whole set of possible conflicts found for the laboratory plant.

Columns  $PC_1$  to  $PC_4$  show the results for the four initial PCs previously obtained. Column  $I_1$  shows the isolation capabilities of first four PCs. Columns  $PC_5$  to  $PC_{15}$  show the additional PCs obtained for the system, and column  $I_2$  shows the isolation capabilities of the approach for the whole set of PCs. Additional rows have been added to the FSM for each of the sensor faults considered. Looking at columns  $I_1$  and  $I_2$ , it is clear that fault discriminability for sensor faults is increased with the new set of additional PCs.

Finally, invoking algorithm 3 we automatically obtain the reduced qualitative fault signature matrix for the plant (see table 6). In this table, columns  $PC_1$  to  $PC_4$  represent the expected deviations (no change (0), or increasing or decreasing (+/-)) in the magnitudes, and in the slope or higher order effects, in the presence of faults. Column  $I$  shows isolation capabilities of this approach. For the sake of simplicity we only show the results obtained for the initial set of four PCs and only for parametric faults.

	$PC_1$	$PC_2$	$PC_3$	$PC_4$	$I$
$C_{T1}$		+*			1
$C_{T2}$		0+	0+		1
$C_{T3}$			+−		1
$R_{V1}$		0−	0+		0
$R_{V2}$		0−	0+		0
$R_{V3}$				+−	1
$R_{pipe}$	+*				1

Table 6: RQFSM found for the laboratory plant.

Comparing tables 4 and 6 it is clear that the RQFSM is better for isolation purposes. A fault in  $C_{T2}$  can now be isolated from a fault in  $R_{V1}$  or  $R_{V2}$  due to the sign in

the derivative. The great advantage of this approach is that using algorithm 3 the RQFSM can be automatically computed for PCs.

## CONCLUSIONS AND FUTURE WORK

In this paper, we have presented an algorithm to automatically compute the set of possible conflicts for a system from its bond graph model. Using the causal structure implied by the topological structure of the bond graph models (obtained through temporal causal graph models that can be automatically derived) greatly facilitates the possible conflicts generation process, because the structure of each PC can be seen as equivalent to a minimal subset of over-determined equations within the TCG, i.e., PCs identify minimal structures in TCGs [Bregon et al. (2008)]

We have proved that explicit inclusion of the observational model of the system in the TCG can lead to additional possible conflicts generation. These possible conflicts does not improve discrimination capabilities of the PCs approach but have proved to be useful to discriminate sensor faults. The proposed algorithms are able to work with this extended TCG and automatically compute the whole set of additional possible conflicts.

Finally, using the temporal relations established in the temporal causal graph, we have proposed an algorithm to compute an extended version of the fault signature matrix for the diagnosis system. This new fault signature matrix, called reduced qualitative fault signature matrix, includes information about the sign in the magnitudes, slopes, and higher order effects. This new fault signature

matrix improves diagnosability of the diagnosis approach for structural faults.

In future work, we will extend our algorithms to compute the set of possible conflicts from hybrid bond graph models. We will also try to test the approach in different and more complex forms of nonlinear systems.

## ACKNOWLEDGEMENTS

Anibal Bregon and Belarmino Pulido's work have been partially supported by the Spanish Ministry of Education and Culture (MEC 2005-08498). Gautam Biswas and Xenofon Koutsoukos' work was partially supported by NASA grants NNX07AD12A and USRA 08020-013.

## REFERENCES

- Bouamama, A. O. and Samantaray, A. K. (2003). Derivation of constraint relations from bond graph models for fault detection and isolation. In *Proceedings of the ICBGM'03*, volume 35, pages 104–109.
- Bregon, A., Biswas, G., and Pulido, B. (2008). Compilation techniques for fault detection and isolation: A comparison of three methods. In *19th Intl. WS. on Principles of Diagnosis, DX'2008*, pages 39–46, Blue Mountains, Australia.
- Cordier, M., Dague, P., Lévy, F., Montmain, J., Staroswiecki, M., and Travé-Massuyès, L. (2004). Conflicts versus analytical redundancy relations: a comparative analysis of the model-based diagnosis approach from the artificial intelligence and automatic control perspectives. *IEEE Trans. Syst. Man Cy. B.*, 34(5):2163–2177.
- Gelso, E., Castillo, S., and Armengol, J. (2008). Structural analysis and consistency techniques for robust model-based fault diagnosis. Technical Report 20, Institut d'Informàtica i Aplicacions, Universitat de Girona.
- Karnopp, D. C., Rosenberg, R. C., and Margolis, D. L. (2000). *System Dynamics, A Unified Approach*. 3rd ed., John Wiley & Sons.
- Koscielny, J. (1995). Fault isolation in industrial processes by the dynamic table of states method. *Automatica*, 31(5):747–753.
- Koscielny, J. and Zakroczymski, K. (2000). Fault isolation method based on time sequences of symptom appearance. In *Proceedings of IFAC Safaprocess*, Budapest, Hungary.
- Mosterman, P. and Biswas, G. (1999). Diagnosis of continuous valued systems in transient operating regions. *IEEE Trans. Syst. Man Cy. A.*, 29(6):554–565.
- Narasimhan, S. and Biswas, G. (2007). Model-based diagnosis of hybrid systems. *IEEE Transactions on systems, man, and cybernetics - Part A: Systems and humans*, 37(3):348–361.
- Puig, V., Quevedo, J., Escobet, T., and Pulido, B. (2005). On the integration of fault detection and isolation in model based fault diagnosis. In *Proceedings of DX'05*, pages 227–232.
- Pulido, B. and Alonso-González, C. (2004). Possible conflicts: a compilation technique for consistency-based diagnosis. *IEEE Trans. Syst. Man Cy. B.*, 34(5):2192–2206.

Reiter, R. (1987). A theory of diagnosis from first principles. *Artificial Intelligence*, 32:57–95.

Roychoudhury, I., Biswas, G., and Koutsoukos, X. (2006). A bayesian approach to efficient diagnosis of incipient faults. In *17th International Workshop on Principles of Diagnosis*.

Samantaray, A. and Bouamama, B. (2008). *Model-Based Process Supervision: A Bond Graph Approach*. Springer Verlag, London, UK.

Samantaray, A., Medjaher, K., Bouamama, B., Staroswiecki, M., and Dauphin-Tanguy, G. (2006). Diagnostic bond graphs for online fault detection and isolation. *Simulation Modelling Practice and Theory*, 14:237–262.

## AUTHOR BIOGRAPHIES

**ANIBAL BREGON** received the M.S. degree in computer science from University of Valladolid, Spain, in 2007, where he is currently a Ph.D. Candidate. His email is [anibal@infor.uva.es](mailto:anibal@infor.uva.es)

**BELARMINO PULIDO** received the Ph.D. degree in computer science from University of Valladolid, Spain. He is Assistant Professor of Computer Science in the Department of Computer Science, University of Valladolid, Spain.

**GAUTAM BISWAS** received the Ph.D. degree in computer science from Michigan State University, East Lansing. He is a Professor of Computer Science and Computer Engineering in the Department of Electrical Engineering and Computer Science, Vanderbilt University, Nashville, TN. His web page can be found at <http://www.vuse.vanderbilt.edu/~biswas>

**XENOFON KOUTSOUKOS** received the Ph.D. degree in electrical engineering from the University of Notre Dame, Notre Dame, IN, in 2000. He is an Assistant Professor in the Department of Electrical Engineering and Computer Science, Vanderbilt University, Nashville, TN. His web page is <http://www.vuse.vanderbilt.edu/~koutsoxd>